

Shipton, Z.K., Evans, J.P., Kirchner, D., Kolesar, P.T., Williams, A.P. and Heath, J. 2004. Analysis of CO₂ leakage through “low-permeability” faults from natural reservoirs in the Colorado Plateau, southern Utah. In: Baines, S. J. & Worden, R. H. (eds.) *Geological Storage of Carbon Dioxide*. Geological Society, London, Special Publications 233, 43-58.

Analysis of CO₂ leakage through “low-permeability” faults from natural reservoirs in the Colorado Plateau, east-central Utah

Z.K. Shipton¹, J.P. Evans², D. Kirchner³, P.T. Kolesar², A.P. Williams², J.E. Heath²

1. Division of Earth Sciences, Centre for Geosciences, University of Glasgow, Glasgow G12 8QQ, Scotland zoeshipt@earthsci.gla.ac.uk
2. Department of Geology, Utah State University, Logan, UT 84322, U.S.A.
3. Department of Earth and Atmospheric Sciences, Saint Louis University, St Louis, MO 63103, U.S.A.

Abstract

The numerous CO₂ reservoirs in the Colorado Plateau region of the United States are natural analogues for potential geologic CO₂ sequestration repositories. To better understand the risk of leakage from reservoirs used for long-term underground CO₂ storage, we examine evidence for CO₂ migration along two normal faults from a reservoir in east-central Utah. CO₂-charged springs, geysers, and a hydrocarbon seep are localised along these faults. These include natural springs that have been active for long periods of time, and springs that were induced by recent drilling. The CO₂-charged spring waters have deposited travertine mounds and carbonate veins. The faults cut siltstones, shales, and sandstones and the fault rocks are fine-grained, clay-rich gouge, generally thought to be barriers to fluid flow. The geologic and geochemical data are consistent with these faults being conduits for CO₂ to the surface. Consequently, the injection of CO₂ into faulted geologic reservoirs, including faults with clay gouge, must be carefully designed and monitored to avoid slow seepage or fast rupture to the biosphere.

Running header: CO₂ leakage through low-permeability faults.

Effective design and implementation of geologic CO₂ sequestration projects require that we understand the storage capacity of a candidate site, the trapping mechanisms for gas, and the hydrodynamics of the system. The CO₂ must be effectively segregated from the atmosphere for periods of thousands of years (Rochelle et al. 1999). Natural sources of CO₂ include mantle degassing, metamorphism or dissolution of carbonates, oxidation or bacterial degradation of organic matter, and thermal maturation of hydrocarbons (Selley 1998). Numerous naturally occurring CO₂ fields contain large amounts of CO₂, providing analogues for the integrity of stored gas systems (e.g. Allis et al. 2001). In some CO₂ fields, however, gas leaks into the atmosphere, primarily along faults. We can study these active leaks to understand the factors that might control the feasibility and safety of future CO₂ injection projects and guide the design and implementation of such projects.

In this contribution we examine the hydrology, stratigraphy, structural geology, and geochemistry of a naturally degassing CO₂ reservoir in the Colorado Plateau of East-Central Utah. The CO₂ discharges from the hydrocarbon-rich Paradox Basin along the Little Grand Wash and Salt Wash faults. These faults cut sandstones, shales, and siltstones producing zones of clay-rich gouge that should theoretically be a barrier to flow (e.g. Freeman et al. 1998). CO₂-charged springs and geysers, travertines (both active and ancient), and carbonate-filled veins are localised along the fault traces. The faults are presently conducting CO₂-rich fluids and the fault has conducted fluids for a substantial amount of time. Abandoned hydrocarbon boreholes are also active conduits for CO₂ to the surface (Doelling 1994; this paper).

In order to quantify the volume of CO₂ that has leaked over the long-term through the Little Grand Wash and Salt Wash faults, the CO₂ sources, pathways, volumes, and rates of flow must be known. We have examined the distribution of the fault-related rocks

and associated outcrop-scale structures of travertines and carbonate veins to characterise the flow paths. We have used the geochemistry of the spring waters, carbonates, and travertines to identify the potential sources of the fluids in the system. We have combined these data to develop a conceptual model for the groundwater/CO₂ flow system (source, pathways, reservoir and cap rocks).

Geological setting

The Colorado Plateau and Four Corners region of the western United States contains at least nine producing or abandoned CO₂ fields with up to 28 trillion cubic feet of CO₂ gas (Allis et al. 2001). Most of these fields are fault-bounded anticlines with four-way anticlinal closure or fault seal along one margin of the field. We focus on the Little Grand Wash and Salt Wash faults, which are at the northern end of the Paradox Basin. The Paradox Basin contains a number of actively producing oil and methane fields, as well as CO₂ fields including the Lisbon field and McElmo Dome field. Immediately south of the study area is the abandoned Salt Wash oil field (Peterson 1973). To the north of the Paradox Basin are the active methane and CO₂ fields of the San Rafael Swell (*e.g.* Drunkards Wash, Ferron Dome). Many of the methane fields in the area produce significant amounts of CO₂ (Cappa and Rice 1995), much of which is vented to the atmosphere.

The Paradox Basin is defined by the extent of organic-rich Pennsylvanian and Permian marine limestones, shales and evaporites (Fig. 1). Hydrocarbon source rocks occur in the Ismay-Desert Creek and Cane Creek cycles of the Paradox Formation (Nuccio and Condon 1995), a mixed sequence of dolostone, black shales, anhydrite, and halite. These are overlain by Triassic and Jurassic fluvial and aeolian redbeds. The oldest lithologies that crop out in the study area are red-brown fine-grained sandstones of the Middle Jurassic aeolian Entrada and Curtis Formations. The Middle Jurassic

Summerville Formation forms characteristic low cliffs with thin bedding and seams of gypsum. The Upper Jurassic Morrison Formation consists of stacked fluvial channels of the Salt Wash Sandstone member, overlain by the bentonite-rich lacustrine shales of the Brushy Basin member. The Lower Cretaceous Cedar Mountain Formation and the Upper Cretaceous Dakota Sandstone are conglomeratic channel sandstones. The youngest formation exposed in the field area is the Upper Cretaceous Mancos Shale, a dark organic-rich marine shale. Approximately 2500 m of Cretaceous and Tertiary rocks have been eroded from the area (Nuccio and Condon 1996).

The Little Grand and Salt Wash faults (Fig. 1) affect the present-day flow of gas and water. Carbonate springs, an active CO₂-charged geyser, and actively forming travertine deposits are localized along the Little Grand Wash fault zone (Baer and Rigby 1978; Campbell and Baer 1978; Doelling 1994) and numerous CO₂-charged springs occur in the region of the Salt Wash faults (Doelling 1994). The faults are part of a WNW trending set of 70 to 80° dipping normal faults in the region. Timing of continued movement along these faults is poorly known, though we present arguments below for Early Tertiary and Quaternary slip. The faults cut the Mancos Shale, consistent with substantial fault activity having occurred at least up to the Middle Cretaceous. The faults cut a north plunging anticline (Figs. 1 and 2), which could be related to salt movement in the Paradox Formation at depth. A basin-wide system of salt anticlines initiated when the salt was loaded by the Pennsylvanian/Permian clastics shed off the Uncompagre uplift to the northeast. Reactivation of the salt-related anticlines and faults occurred during Laramide (Eocene) contraction (Chan et al. 2000).

The Little Grand Wash fault

The Little Grand Wash fault is a south-dipping arcuate normal fault with a surface trace length of 61 km (Fig. 1). The Little Grand Wash fault consists of two parallel strands

from 3.2 km east to 0.1 km west of the Green River; elsewhere it has only one strand (Fig. 3). Total vertical separation on the fault near the Green River is 180 to 210 m, most of which is accommodated by the southern fault strand. The two strands of the fault were encountered at depth in an abandoned well (Amerada Hess, Green River no. 2 drilled in 1949, total depth 1798 m) at 805 m and 970 m. Drilling records state that the deeper of the two faults has Cutler Group sediments in the hanging wall and Hermosa Group sediments in the footwall. It is therefore unclear what the offset of the fault is at this depth, or whether the fault cuts the Paradox Formation (Fig. 2).

The fault is cut by several stream channels that provide excellent cross-sectional exposures of the fault zone and associated host-rock alteration. Between the two main strands of the fault, smaller faults define structural terraces with varying dips (Fig. 4a). Slickenlines on subsidiary fault surfaces indicate mostly dip-slip with some oblique left- and right-lateral movement. The fault zone contains 70 cm to 3 m of foliated clay gouge with occasionally well-defined, sub-planar slip-surfaces (Fig. 4a). Smaller faults with offsets less than 1 m are decorated with a thin (mm-thick) foliated purple-black, clay-rich fault gouge and occasional thin calcite veins (1-2 mm thick) with sub-horizontal fibres. The normally dark purple-red Summerville Formation is bleached to a pale yellow for up to several metres into the footwall. This alteration is localised along the subsidiary faults and within certain beds.

CO₂ emissions and springs

Several active CO₂-charged springs are localised along the two strands of the Little Grand Wash fault zone (Fig. 3). The Crystal Geyser erupts to heights of up to 25 m at 4 to 12 hour intervals (Fig. 5a). This is not a geyser in the strict sense of the term; the water in the geyser is cool and the eruptions are powered by CO₂-charged waters rather than a heat source. The geyser began erupting when the Glen Ruby #1-X well was

drilled in 1935. This abandoned exploration well was completed to the base of the Triassic section (TD 801 m). Occasionally the geyser water has a strong sulphur smell, and/or a thin film of hydrocarbons coating the water pooled around the drill pipe. The driller's records document that the well was spudded into a travertine mound and that the travertine thickness was 21.5 m before hitting bedrock (Baer and Rigby 1978). The spring system must have been active prior to the well being drilled.

Anecdotal reports and scant completion records indicate that the geyser erupted more regularly (at 11 hour intervals) in the past. The hole is currently open to ~130 m depth. Much damage is reported to have been done to the borehole, including dynamiting of the hole, attempts at cementing, and dumping of railroad ties. CO₂-charged emissions continue despite this damage. A 1.5 m high steel pipe was added to the top of the well casing in 2001. This pipe has had no discernable effect on the geyser's eruption.

Three other springs are located on the system of travertine mounds around the geyser. To the northeast a water-filled pool and a chocolate-brown, mud-filled pool erupt penecontemporaneously with the geyser. These are located on the back of the travertine mound where it has been badly damaged by vehicles. To the north, another small water-filled pool is located on the active travertine slope. The close correlation of the timing of the geyser and activity of these springs suggest that the latter either reflects some escape of the CO₂-charged waters from the well bore at shallow levels, or that these pools could be the original, pre-well flow paths for the CO₂-charged waters to the surface. It is common for hydrothermal travertine spring sources to switch locations when the flow paths become cemented (Chafetz and Folk 1984). Although in this cool water system, cementation may not be as rapid as in hydrothermal systems, it is still likely that the flow paths switch with time when they become sealed by calcite precipitation.

Within the Green River, small gas seeps produce small streams of bubbles. These can be observed on both banks of the river and are parallel to the trace of the fault. A kilometre to the east of the Crystal Geyser, in a low-lying area between the two fault strands, gas seeps audibly from the ground (Fig. 3). A small amount of water flows sporadically from upstream of this location leaving salty deposits and wet sand in the base of the wash. Further to the east, an oil seep is located on the southernmost fault strand (Fig. 3). A shallow pit contains fresh oil indicating that there is active flow of petroleum to the surface. The outcrop close to this seep (Salt Wash member of the Morrison Formation) contains patches of oil staining.

Mineral deposits

Modern travertines at the little Grand Wash fault consist of bedded travertine mounds that were deposited from the Crystal Geyser and surrounding springs (Fig. 5). The surface of the active geyser mound has a classic rimstone texture (Fig. 5c) and lobes of travertine have built out to form sub-metre scale caves with stalactites. An ochre colour indicates a small component of iron oxide. These travertines successively bury the vegetation that surrounds the geyser. The travertine surface has regions of actively forming and inactive travertines, presumably controlled by switching of the source spring location or by lateral migration of flow across the surface of the mound.

To the southwest of Crystal Geyser, older carbonate deposits are in the process of being covered by the present day mound. These deposits are in the form of two distinct mounds of carbonates and breccias, one at the level of the river cutting an older one to the east (Figure 5a). From a distance, it appears as though variably dipping veins are visible within these mounds, though these are not veins in the usual structural geological sense. They consist of cm-thick to tens of cm-thick sub-horizontal tabular masses of radiating acicular calcite and aragonite crystals 6 to 15 cm long with botryoidal or

mammilated top surfaces (Fig. 5b). Fresh surfaces are bright white, with occasional pale yellow banding. These veins often have paired banding and/or mammilated surfaces, which face toward the centre of the vein. Deposits of this form (described as ray-crystal crusts by Folk et al. 1985) have been interpreted to form underwater, with the apex of the radiating crystals pointing towards the source of fluids (*i.e.*, in the centre of the veins). Occasionally the centre of these veins contain stalactite-like structures suggesting that sub-horizontal fissures were in-filled above the water table. Above these deposits lie travertine-cemented breccias that includes clasts of ray-crystal calcite and sandstone clasts. The surfaces of the inactive mounds have some rimstone textures preserved, though they have been extensively damaged by vehicles. The 1867 Powell expedition documented “satin spar” at this location (Powell, 1895), which we interpret to be either the travertine terraces or the bright white ray-crystal calcite veins.

Other ancient travertine deposits along the fault are at higher elevations (up to 37 m, Baer and Rigby 1978) than the one presently forming. These deposits tend to form resistant caps to small buttes. The hangingwall of the fault in Figure 4a contains a thicker ancient travertine deposit than the footwall, though it is unclear if this deposit filled in the space left by faulting or if movement on the fault cut a pre-existing deposit. The ancient travertines consist of dense-bedded layers, 1 to 2 mm thick, interbedded with vuggy open carbonate 1 to 3 cm thick. Horizontal and vertical carbonate ray-crystal veins up to 30 cm thick cross cut these deposits. In an outcrop east of the Geyser, an impressive array of mm- to cm-thick veins with a boxwork pattern has completely obliterated the original fabric in the fault gouge (Fig. 4b). The veins in this array are not parallel to the original fault-parallel gouge fabric. This boxwork is cross cut and offset by thicker sub-vertical veins with occasional stalactite textures.

The variation in the locations of the inactive deposits shows that the loci of active effusion of CO₂-rich waters have changed in the past. The carbonate mounds predominantly form between the two strands of the Little Grand Wash fault, or at structurally complex areas such as stepovers between the fault strands. The spatial correlation of the ray-crystal calcite/aragonite veins and the travertines is consistent with the latter having been the “plumbing system” to the travertines.

The Salt Wash faults

The Salt Wash faults (sometimes termed the Tenmile Graben) are a set of N 70° W striking normal faults. The map-scale structure of the faults reveals two normal fault systems that form a shallow graben over 15 km long (Fig. 1). The faults offset Jurassic Entrada Sandstone in their footwalls against Cretaceous and Jurassic Cedar Mountain Formation in the centre of the graben. The Salt Wash faults consist of two linked en echelon graben segments (Doelling 2001) and may be structurally linked to the Moab fault system to the southeast (Fig. 1), though Quaternary deposits obscure the area where this linkage potentially occurs. The depth to which these faults extend is uncertain (Fig. 2), but they may sole into the Paradox salt sequence, and could be related to salt tectonics in the region. We have studied in detail two areas along the northernmost Salt Wash fault - the Tenmile Geyser and Torrey’s spring areas (Fig. 6).

Tenmile Geyser

The Tenmile Geyser is centred on an abandoned well 200 m into the hanging wall of the northern fault (Figure 7a). A drill pipe sits within a low mound of flaky travertine with poorly developed rimstone textures. The Tenmile Geyser erupted infrequently in the past (Doelling 1994) and continues to erupt with infrequent 1 to 1.5 m high eruptions. A second mineral-charged spring sits on a low mound 100 m into the footwall of the fault. There is anecdotal evidence that a set of travertine terraces with rimstone textures used

to exist at this locality. This mound has since been excavated into a pit about 2 by 3 m in size and 1.5 m deep. The bottom of this pit does not reach the base of the travertine deposit. There is an almost constant stream of CO₂ from three vents in the base of the pool, but this spring has not been documented to have geyser-style eruptions.

There are extensive inactive travertines up to 4 m thick at elevations up to 30 m above the level of the present-day spring, some with well-developed rimstone textures. These travertines are presently being quarried. A two to 10 m thick zone of fractures, intense alteration, and veining obliterates the primary sedimentary structures beneath portions of the travertine deposits. Two to five cm-thick bedding parallel carbonate veins extend up to 50 m away from the fault zone. In some places mammilated ray-crystal veins change from vertical to horizontal orientation within the outcrop. These occasionally contain open vuggy deposits with rhombohedral calcite crystals, interpreted as forming in subaerial or spelean pools. Fractures up to two metres deep that cut the mounds have been filled with bedded travertine. The travertines tend to form resistant caps to a line of small buttes along the fault trace. All the travertines along the Salt Wash faults are localised either on the northernmost fault trace or in the footwall of this fault. The only activity seen within the graben is the Tenmile Geyser.

The fault gouge is locally well-exposed, and consists of a zone up to 5 m thick of slices of lithologies separated by clay-rich foliated gouge (Fig. 7b). In the footwall north of the Tenmile Geyser, the Entrada Sandstone (usually red) has been extensively bleached to a light tan to pale yellow. In other places along the fault zone, the Entrada Formation is bleached in zones close to the fault and along fractures (Fig. 7c). Close to the fault, poikilotopic aragonite cements occur preferentially in certain horizons of the host rock.

Torrey's spring

This spring occurs in the Entrada sandstone in the footwall to the northern fault (Figure 6). The spring is located in the centre of a fresh-looking travertine mound about 15 m in diameter, which has slope of $\sim 8^\circ$. The saline spring bubbles almost constantly and occasionally smells of sulphur. To the authors' knowledge, it has never erupted in geyser-style eruptions. This spring appears to be close to the location of the Delaney Petroleum Corporation #1 drill hole drilled in 1949, which had a total depth of 299 m. There was no oil show in this well.

The spring was first visited by the authors in June, 2000, and again in June, 2001. During this interval, the travertine had advanced significantly over a large area and had created a small travertine "frozen waterfall" into a dry river bed to the west. This is evidence of the rapid growth rate of these travertine mounds and the high CaCO_2 content of the effusing waters. Growth rates of 10 cm to 1 mm per year have been documented in other travertine deposits, though these were areas of warm or hot water deposition (Folk et al. 1985).

The main Salt Wash fault outcrops to the south of Torrey's spring. A line of small buttes (10 to 20 m high) capped with travertines parallels the location of the fault. Commonly, the steeply dipping veins are larger than, and cross cut, the sub-horizontal veins. Fissures have been infilled with travertines, and the infill breccias contain fragments of the vein material. These outcrops also contain gypsum, though it is unclear if they are associated with the fault or if they are from the original host rock (Entrada Sandstone). Alteration of the host rock to pale yellow "bleached" sandstone is focused along fractures close to the fault (Fig. 7c). Bedding parallel calcite veins 2 to 5 cm thick extend up to 350 m from the fault in the footwall.

Water Chemistry

We collected and analysed the chemistry of waters from the Crystal Geyser on the Little Grand Wash fault, and from two CO₂-charged springs along the Salt Wash fault (Torrey's spring and the excavated spring at Tenmile geyser). Water samples were collected in polyethylene bottles and samples for cation analyses were acidified with reagent-grade nitric acid to a pH of 2 or less. Field analyses included pH and temperature. Field alkalinity was not determined in the field, but relatively low balance errors for the analyses show that this did not cause significant error. Samples were kept refrigerated until analyzed for major element composition. Table 1 presents the chemical data.

Dissolution of calcite cannot account for all of the CO₂ in the water because there is substantially less calcium in the water than bicarbonate. There must be an alternative or additional source for the CO₂. Similarly, the excess sodium in the waters (Cl⁻/Na⁺ ratios range between 0.6 and 0.8 for Crystal geyser system waters) could not be solely from the dissolution of halite and therefore must be derived from other minerals such as Na-bearing montmorillonite. The water we collected from the main Crystal Geyser is supersaturated with respect to calcite, aragonite, and dolomite (Table 2). Modelling of our data and the water chemistry of Mayo (1991) with the programme Wateq (Truesdel and Jones 1974) indicates that the Crystal Geyser water is supersaturated with respect to aragonite, calcite, dolomite, fluorite, and gypsum (Table 2). This suggests that the fluid source for the veins could have had a similar composition to present-day fluid.

Results of modelling with Salt Norm (Bodine and Jones 1986) are consistent with the chemistry of the geyser water being a mixture of meteoric water and brine from redissolved marine evaporites. For a given water analysis this program calculates the salt composition that would result if that water were evaporated to dryness. The water

composition will reflect the materials with which the water came in to contact; therefore the calculated salt composition can provide clues about the composition of those materials. Bodine and Jones (figure 4, 1986, p.37) list criteria that define water types based on the calculated salt composition. Applying those criteria to our water samples suggests that the water in the Crystal Geyser system primarily is a mixture of redissolved marine evaporites and meteoric water (Table 3). Evaporites occur in the Paradox salt, and also in shallower units such as the Carmel Limestone and Summerville Formation.

Water chemistry was monitored during two separate Crystal Geyser eruptions to see what chemical changes occur during an eruption cycle. There were larger changes in water chemistry for the longer eruption (30 minutes as opposed to less than 10 minutes) consistent with an influx of relatively low salinity groundwater recharging the well bore during an eruption (Figure 8).

Isotope data

Samples of carbonate veins and travertine were analysed in the stable isotope laboratory at Saint Louis University using both continuous-flow and conventional techniques. For continuous flow analysis, submilligram aliquots of sample powder were digested in orthophosphoric acid at 90 °C for several hours in an automated extraction device. Liberated gas was entrained in a helium stream, passed through a GC column for isolation of the CO₂ and then transferred on-line to a gas-source, isotope-ratio mass spectrometer. Duplicates and some triplicate analyses were made for most samples. Most of the samples were also analyzed by conventional (manual) techniques following the lab procedure described in Kirschner et al. (2000). The average values of these analyses are depicted in Figure 8a. Carbonate standards (two in-house standards) were

analyzed with the samples. Analytical precision of $\delta^{13}\text{C}$ was below 0.10‰ (N=23; 1σ); $\delta^{18}\text{O}$ was below 0.26‰ (N=20 excluding one set of 3 standards; 1σ).

Several trends can be observed in the data (Fig. 9a). Travertine data from individual localities lie on subvertical trends. In contrast, most ray crystal calcite/aragonite veins have lower $\delta^{18}\text{O}$ and similar or lower $\delta^{13}\text{C}$ values relative to the travertines from the same localities (dashed trends in Fig. 9a). The $\delta^{18}\text{O}$ values are consistent with precipitation of the carbonate at low temperature (ca. 15 to 35 °C) from water with a $\delta^{18}\text{O}$ value less than -7‰, consistent with partly evolved (isotopically altered) meteoric water being an important component of the water in the faults and geysers (cf. IAEA 2001). The variation in $\delta^{18}\text{O}$ values among sites could be due to variable mixing of meteoric water with other fluids or partial exchange with carbonate rocks or CO_2 at depth.

The vertical $\delta^{13}\text{C}$ trend of the travertines is consistent with CO_2 degassing during discharge and surface flow of the spring water. Light isotopes of carbon and oxygen preferentially fractionate into the gas during degassing resulting in an appreciable increase in carbon isotope values of the dissolved inorganic carbon. Although the same phenomenon is occurring for the oxygen isotopes, the resulting shift in isotopic values is not large due to the overwhelming abundance of oxygen in the water. Similar trends have been documented in other studies of travertine deposits and associated spring waters (Fig. 9b and references therein).

The positive increase in $\delta^{18}\text{O}$ and $\delta^{13}\text{C}$ values between veins and travertines from individual sites is most likely associated with increased isotopic fractionation due to cooling of water during upward migration and surface discharge. Assuming the water is cooling as it is ascending and there is an abundance of fluid in the system, then isotopic

values of carbonates precipitating from cooler water will be higher (heavier) for both carbon and oxygen, resulting in a positive $\delta^{18}\text{O} - \delta^{13}\text{C}$ trend. Evaporation of the water could also have produced the positive trend. If a significant amount of water is evaporating, then the water that remains becomes isotopically heavier (because water molecules with the lighter isotopes preferentially evaporate). Carbonates precipitated from water that has undergone significant evaporation will consequently have higher (heavier) oxygen isotopic values (and carbon values, assuming that CO_2 is degassing at the same time). Either mechanism can produce positive trends.

Discussion

In order to evaluate the effectiveness of the Little Grand Wash and Salt Wash faults as conduits for leakage of CO_2 we ideally need to know the source of the CO_2 , the volume of the gas reservoir, and the rate at which this reservoir is being depleted. Although our work is still in its initial stages, the preliminary results can be used to build a working model for the source, pathways, and timing of flow in the Little Grand Wash and Salt Wash fault system.

Source of CO_2

A number of processes can produce CO_2 within basins including mantle degassing, metamorphism or decarbonation of carbonates, oxidation and/or bacterial degradation of organic matter, and maturation of hydrocarbons (Selly 1998). Helium isotope data of gas from the Crystal Geyser and a spring on the Salt Wash fault suggests only a minor component of mantle-derived helium (Heath et al. 2002, Heath 2004), thus excluding a mantle source for the CO_2 . The gas in the Paradox basin is therefore likely to be sourced from one or more of the remaining processes, though this source can not be unequivocally identified solely from the carbon and oxygen isotope data of the

carbonates or water chemistry. It is clear that the $\delta^{13}\text{C}$ values of +4 to +5‰ for the veins are probably more closely associated with the subsurface fluid than the higher $\delta^{13}\text{C}$ values of the travertine samples. Barring the presence and dissolution of carbonates with unusually high $\delta^{13}\text{C}$ values in the basin, two probable sources of isotopically heavy CO_2 in the field area are 1) biologically mediated hydrocarbon generation, and 2) thermally induced decarbonation of carbonates.

Many previous studies have focussed on existing oil and gas deposits in the Paradox Basin (Hansley 1995; Nuccio and Condon 1995), and on the evidence for a palaeo-hydrocarbon play in and around the Moab fault (Chan et al. 2000; Garden et al. 2001). The presence of the oil seep at the Little Grand Wash fault suggests that the fault is acting as a conduit for oil as well as CO_2 . The geochemistry of the oil may be consistent with it coming from Lower Permian Formations (P. Lillis pers. comm. 2001), which are the source of much of oil in Upper Palaeozoic rocks of the northern and central Rocky Mountains (Claypool et al. 1978). Sanford (1995) concluded, however, that the Permian was an unlikely source rock for hydrocarbons in the Paradox basin based on a study of palaeo-groundwater flow in the White Rim Sandstone, which has been bleached by hydrocarbon-bearing reducing fluids (Hansley 1995). Alternative hydrocarbon source rocks in the area include the late Proterozoic Chuar group, the Mississippian Chainman shale, the Lower Triassic Sinbad Limestone, and shales within the Paradox Formation. Although isotopically light $\delta^{13}\text{C}$ values of hydrocarbons and associated CO_2 are the norm for hydrocarbon deposits (e.g., Schoell 1983), it is possible for hydrocarbon-associated CO_2 to have isotopically heavy $\delta^{13}\text{C}$ values due either to biologically mediated reactions (e.g., Coleman et al. 1988; Jenden et al. 1988) or to low-temperature carbon isotope exchange between hydrocarbons and CO_2 . Neither can be excluded with the present data set.

A more probable source of isotopically heavy and abundant CO₂ is the thermal decarbonation of carbonates (cf. Baumgartner and Valley 2001). Cappa and Rice (1995) presented evidence that some of the CO₂ in the gas fields of southern Utah and Colorado was produced by high-temperature thermal decomposition of the Mississippian Leadville Limestone or decomposition of kerogen within the Leadville Limestone or the Paradox Formation. We suggest that this may have occurred within the contact aureoles of Tertiary intrusions (the La Sal and Henry mountains). Both the Leadville Limestone and the potential hydrocarbon source rocks lie within or below the Paradox Formation. Therefore, regardless of the source of CO₂, it is clear that the CO₂ must have migrated through the salt.

Timing of fluid flow

The ancient travertine terraces and veins preserved at Little Grand Wash and Salt Wash demonstrate that the faults have been the focus of CO₂-charged waters for a substantial amount of time. Although many of the springs in the area are due to recent drilling activities, there continues to be flow from springs and gas seeps that are not associated with wells. The flow at the Crystal Geyser was active prior to 1935, when the Ruby 1-X well was drilled, and is likely to have produced the deposit that was observed by the Powell expedition in 1867. The rest of the drilling-associated springs have only poorly developed (incipient) travertine mounds. Deposits of travertine at least as thick as those at the Crystal Geyser occur in areas where no drilling has occurred. The various ancient travertines are evidence that the migration pathways within and next to the fault zones have switched over time.

Some of the ancient travertines are located up to 37 m above the level of the present day springs. Assuming that they were not initially deposited at the tops of the buttes, the amount of incision could be used to infer the age of the travertines. Baer and Rigby

(1978) suggested a date of 200,000 years for the highest-level inactive travertines based on Colorado Plateau uplift rates. The uplift rate on the Colorado Plateau is currently a focus of debate, however, it is obvious that these spring systems have been active for a substantial amount of time.

Timing of fault activity

Although we do not yet have geochronologic constraints on the age of activity on the Little Grand and Salt Wash faults, structural relations between faults and travertine deposits are consistent with recent fault movement. Travertine filled fractures within the ancient travertine deposits could be related to seismic events (cf. Hancock et al. 1999). Some of the travertines appear to be nestled within a hanging wall half-graben, suggesting that a scarp existed at the time of travertine deposition. This could be the result of differential erosion of the relatively soft Mancos shale in the hanging wall, or due to syn-depositional movement along the faults. Quaternary activity has been reported along the Salt Wash fault (Hecker 1993). These faults may be related to movement of the Paradox salt, which has resulted in numerous episodes of fault motion southeast of our study area (Chan et al. 2000; Garden et al. 2001). Pevear et al. (1997) used K-Ar techniques on fine-grained illite of the Moab fault to show that this fault was active between 60 to 50 Ma consistent with one of the regional episodes of salt movement and dissolution (Chan et al. 2000; Garden et al. 2001).

Flow paths for CO₂ and water

All except one of the potential sources of CO₂ are below the Paradox salt. The Paradox salt is an interbedded unit with halite beds up to several metres thick. Salt can deform by crystal-plastic deformation at high strain rates, which can result in rapid healing of faults. Therefore faults that cut salt are not usually considered to be conduits for fluid flow unless faulting forms a juxtaposition of non-salt rocks between the hanging wall

and footwall. From driller's records of wells in the study area, the thickness of the salt below the Little Grand Wash fault is of the order of 650 to 1300 m but the fault offset is only ~200 m. Thus flow along the faults is the likely pathway through the salt.

Given the clay-rich nature of the fault zones within the Jurassic and Cretaceous sequences we would generally expect a low-permeability fault rock. However, the localisation of springs and travertines, the presence of hydrocarbon seeps along the Little Grand Wash fault, and the close association of faulting and bleached sandstones (this study; Chan et al. 2000; Garden et al. 2001) suggests that there is a component of up-dip flow within or adjacent to these fault zones. Outcrops of the fault show that the foliated fault gouge has a strong fabric anisotropy, and that in places slip is localised onto discrete slip surfaces. This fabric anisotropy will result in anisotropy in fault gouge permeability. Specifically, it is likely that the permeability is substantially higher along the fault surface than in the cross-fault direction.

Regional aquifers that could act as reservoirs for the CO₂ include the Entrada Sandstone, the Navajo/Wingate sandstones and the White Rim sandstone. The water temperature (18°C) indicates that shallow aquifer waters are producing the springs, unless slow upwards flow rates allow thermal equilibration with the surrounding rocks. Heat flow values in the Green River area are consistent with geothermal gradients of 34°C km⁻¹ (Nuccio and Condon 1996) suggesting that the Navajo-Wingate aquifer (200 to 450 m below the footwall to the Little Grand Wash fault) is the reservoir for shallow groundwater that is being charged with deep CO₂.

Several other CO₂-charged springs occur in this region. The once spectacular Woodside Geyser, situated at the old town of Woodside approximately 40 km north of the study area, now only erupts sporadically to a few meters from an abandoned drill hole. The Tumbleweed and Chaffin Ranch geysers erupt occasionally from drill holes to the south

of the faults in this study (Fig. 2). These geysers, and the springs along the faults generally fall along the line of the regional north-plunging anticline axis (Fig. 2). This suggests that the flow of CO₂ or CO₂-charged fluids is focused along the anticline axis. The active springs along the Little Grand Wash and Salt Wash faults all occur in the footwall, apart from the Tenmile Geyser, where the host drill hole may well penetrate the fault. It is possible that the fault is acting as a barrier to regional south-directed groundwater flow in the Navajo/Wingate aquifer (Hood and Patterson 1984), concentrating the CO₂-charged fluid in a footwall reservoir. The fault would be contributing to the flow path through the impermeable layers above the aquifer (the Carmel limestone, Morrison Formation etc.). In this case, the fault has higher up-dip permeability than cross-fault permeability. The travertines are generally located at structural complexities along the fault zone, such as at the ends of segments or at stepovers. This relationship is commonly observed in hydrothermal systems (Curewitz and Karson 1997; Hancock et al. 1999).

The bleaching and euhedral aragonite cements that are found in the footwall host rock close to the faults are evidence that fluid infiltrated the host rock as well as simply being channelled up the fault. Chan et al. (2000) and Garden et al. (2001) suggest that such bleaching is the result of movement of a reducing fluid through the system. They argue that this was meteoric water driven by topographic flow to salt depth where the fluid becomes saline and reducing and reacted with hydrocarbons. They argue for fault-controlled upward flow and movement of the fluid out into the Jurassic aquifer sequence.

Implications for CO₂ Sequestration projects

The preliminary results of this study have implications for the design of CO₂ sequestration projects. These projects require that CO₂ be isolated from the atmosphere

on a timescale of hundreds to thousands of years (Rochelle et al. 1999). It is clear that the Little Grand Wash and Salt Wash faults have been conducting fluids for a substantial period of time; however, more work remains to be done on the Little Grand Wash and Salt Wash faults to evaluate the fraction of the total CO₂ reservoir that is leaking from the faults. A relatively low volume leakage of a large reservoir may well be deemed acceptable in a large sequestration project. The volume of carbon that is trapped in carbonate deposition at the surface must be estimated from future mapping of the total volume of travertines and carbonates around the wells and springs. The fact that many of the springs in the region are centred on abandoned oil wells suggests that care should be taken with well-bore integrity during the design and monitoring of CO₂ sequestration projects.

As suggested by the correlation of CO₂ degassing and earthquake faults, the stress state in and around faults may significantly influence whether a fault is conductive or not (Barton et al. 1995). Zoback and Townend (2001) suggest that many faults in the crust are critically stressed in that they are very near the point of failure as predicted from a Mohr-Coulomb failure analysis. Present-day seismicity in the Colorado Plateau is dominated by extension along northwest to north-northwest striking normal faults (Wong and Humphrey 1989) and the present state of stress in the region is consistent with north-northeast extension (Mueller et al. 2000). The Little Grand Wash and Salt Wash faults are therefore optimally oriented for failure in the present stress field and are likely conduits for the upward migration of fluids. Therefore, in addition to mapping the occurrence of faults in the vicinity of potential CO₂ disposal sites, the orientation of faults with respect to the current stress state should be taken into account. Given the possibility of Quaternary to Recent fault activity, it is possible that seismic activity could have had a part to play in the migration of the CO₂ to the surface; earthquake activity

has often been correlated with outgassing of CO₂ reservoirs (Irwin and Barnes 1980; Sugisaki et al 1983; Chiodini et al. 1995; Guerra and Lombardi 2001) and there is often a link between earthquakes and the activity of geothermal geysers.

The Little Grand Wash and Salt Wash faults cut rocks that are good analogues for low net-to-gross reservoir rocks such as those found in the North Sea. The sealing capacity of faults depends on the type of structures that occur in the fault zone, how they are arranged, the contribution of each structure type to flow, and geochemical processes in the faults, which may add or remove sealing capacity. Due to the poor preservation potential of faults in outcrops of shale-rich rocks, few field analogues have been studied in detail. Consequently, there is little data with which to make predictions regarding the behaviour of these faults. Such faults are often accounted for in hydrocarbon reservoirs using simple shale smear or gouge algorithms (e.g. Freeman et al. 1998). These make substantial assumptions about the fault, specifically that the seal is formed by physical smearing or mixing of the low permeability clays in the host rock with no diagenesis of the fault rocks. Fault rock alteration and diagenesis is clearly taking place in this locality and would almost certainly take place within any CO₂ sequestration schemes that included faults. It is clear that much further work needs to be done on such systems before the implications for long-term storage of CO₂ can be fully understood.

Conclusions

The Little Grand Wash and Salt Wash faults, east-central Utah, affect the present-day CO₂-charged groundwater flow regime over reservoir-scale distances. The CO₂ flows upward from one or more deep sources that include the thermal decarbonation of carbonates deep in the basin and/or microbially mediated hydrocarbon generation. Most of the potential CO₂ source rocks are below or within the Pennsylvanian Paradox Formation, approximately 1.5 km below the surface. Observations of fault-controlled

cementation, bleaching, and hydrocarbon accumulation elsewhere in the basin suggest that faults have been a conduit for reducing fluids and hydrocarbons. It is therefore likely that faults have been a conduit for deep-sourced CO₂ through the Paradox salt and other low-permeability rocks in the basin.

The low temperature of the water that effuses at the springs and geysers suggests that it is sourced from the shallow Navajo/Wingate aquifer. The units that provide top seals to this aquifer are the Jurassic Summerville and Morrison Formations. The Cretaceous Mancos Shale and Cedar Mountain Formation would provide a juxtaposition seal in the hangingwall to the faults. The location of well-bore-related springs in the area show that gas-charged groundwater is ponded at the apex of a regional north-plunging anticline. Both natural and drill hole-related spring and travertine activity is concentrated along the fault zones, specifically in the northern footwalls. This suggests that the faults have a relatively low cross-fault permeability and form a seal to migration of gas up the plunge of the anticline. The faults must therefore be the conduit for the gas to move through the sealing units, and have relatively high hydraulic conductivity in the vertical (up-dip) direction. The gas either seeps upward continually or is transported during fault slip events. The springs and travertines are concentrated at structural complexities and linkage zones along the faults.

The long-lived nature of the fluid flow is demonstrated by ancient travertines and vein systems that are localized along the fault zone. The faults cut rocks that are analogous to the North Sea reservoirs in which it is proposed to dispose of significant quantities of CO₂. Even if a relatively small proportion of the gas reservoir is able to escape along fault zones, then over periods of hundreds to thousands of years the efficiency of CO₂ sequestration projects could be called into question. We have determined the basic regional structure of the Little Grand Wash and Salt Wash fault system, making these

faults an ideal candidate for a more detailed study of the interaction between fluids and low-permeability faults in clay-rich rocks at the oil-field scale.

Acknowledgements – Thanks to Bill Shea for introducing us to the field site, and to Torrey Copfer for discovering some of the studied springs. This work was funded in part by the CarbonCapture Project, a joint industry-government consortium. Steve Laubach, Tim Needham and Richard Worden provided thoughtful reviews of the manuscript. We thank Scott Imbus for insights into the geochemistry of petroleum systems, and to Craig Lewis and Shelaigh Baines for organizing the 2001 session on CO₂ at EUG. We thank the people of Green River, Utah who provided information on historical eruptions of the Crystal Geysir.

References

- Allis, R., Chidsey, T., Gwynn, W., Morgan, C, White, S., Adams, M., and Moore, J., 2001, Natural CO₂ reservoirs on the Colorado Plateau and southern Rocky Mountains: candidates for CO₂ sequestration. In proceedings of the National Energy Technology Laboratory, first national conference on carbon sequestration, World Wide Web address:http://www.netl.doe.gov/publications/proceedings/01/carbon_seq/6a2.pdf
- Amundson, R.G. and Kelly, E. 1987. The chemistry and mineralogy of a CO₂-rich travertine depositing spring in the California Coast Range. *Geochimica et Cosmochimica Acta*, **51**, 2883-2890.
- Baer, J.L., and Rigby, J.K. 1978. Geology of the Crystal Geyser and the environmental implications of its effluent, Grand County, Utah. *Utah Geology* **5**, 125-130.
- Barton, C.A., Zoback, M.A., and Moos, D. 1995. Fluid flow along potentially active faults in crystalline rock, *Geology*, **23**, 683-686.
- Baumgartner L.P., and Valley J.W. 2001. Stable isotope transport and contact metamorphic fluid flow: In: J.W. Valley and D.R. Cole (eds) *Stable Isotope Geochemistry, Reviews In Mineralogy and Geochemistry*, 43:415-468.
- Bodine, M.W. and Jones, B.F. 1986. The Salt Norm: A quantitative chemical-mineralogical characterization of natural waters. *U. S Geological Survey Water Resources Investigations* **86-4086**, 130 p.
- Campbell, J.A. and Baer, J.L. 1978. Little Grand Wash fault-Crystal Geyser area. In: J.E. Fasset and Thomaidis N.D. (eds) *Oil and gas fields of the Four Corners area*. Four Corners Geological Society, 666-669.

- Cappa, J. A. and Rice, D.D. 1995. Carbon dioxide in Mississippian rocks of the Paradox Basin and adjacent areas, Colorado, Utah, New Mexico and Arizona. U.S. Geological Survey Bulletin 2000-H, 21pp.
- Chafetz, H.S., and Folk, R.L. 1984. Travertines: Depositional morphology and the bacterially constructed constituents, *Journal of Sedimentary Petrology*, **54**, 289-316.
- Chafetz, H.S., Utech N.M., Fitzmaurice S.P. 1991a. Differences in the $\delta^{18}\text{O}$ and $\delta^{13}\text{C}$ signatures of seasonal laminae comprising travertine stromatolites. *Journal of Sedimentary Petrology* **61**, 1015-1028.
- Chafetz, H.S., Rush, P., Utech, N. 1991b. Microenvironmental controls on mineralogy and habit of CaCO_3 precipitates: an example from an active travertine system. *Sedimentology* **38**, 107-126.
- Chan, M.A., Parry, W.T., Bowman, J.R. 2000. Diagenetic hematite and manganese oxides and fault-related fluid flow in Jurassic sandstones, southeastern Utah. *American Association of Petroleum Geologists Bulletin*, **84**, 1281-1310.
- Chiodini, G., Frondini, F. and Ponziani, F. 1995. Deep structures and carbon dioxide degassing in Central Italy. *Geothermics*, **24**, 81-94.
- Claypool, G. E., Love, A. H., Maughan, E.K. 1978. Organic geochemistry, incipient metamorphism, and oil generation in black shale members of Phosphoria Formation, Western Interior United States. *American Association of Petroleum Geologists Bulletin*, **62**, 98-120.
- Coleman, D.D., Liu, C.-L. and Riley, K.M. 1988. Microbial methane in the shallow Paleozoic sediments and glacial deposits of Illinois, U.S.A. *Chemical Geology* **71**, 23-40.

- Curewitz D. and Karson J.A. 1997. Structural settings of hydrothermal outflow; fracture permeability maintained by fault propagation and interaction. *Journal of Volcanology and Geothermal Research*. **79**, 149-168.
- Doelling, H. 1994. Tufa deposits in western Grand County. *Survey Notes - Utah Geological Survey*. **26**. 8-10, 13.
- Doelling, H. 2001, The Geologic map of the Moab and eastern San Rafael Desert 30x60' quadrangles. Utah Geol. Surv. Map M-180.
- Freeman, B., Yielding, G., Needham, D.T., and Badley, M.E. 1998, Fault seal prediction: The gouge ratio method. In: Coward, M.P. Daltaban, T.S., and Johnson, H. (eds), *Structural Geology in Reservoir Characterization*, Geological Society of London Special Publication **127** 19-26.
- Friedman, I. 1970. Some investigations of the deposition of travertine from Hot Springs – I. The isotopic chemistry of a travertine-depositing spring. *Geochimica et Cosmochimica Acta* **34**, 1303-1315.
- Folk, R.L., Chafetz, H.S., Tiezzi, P.A. 1985, Bizarre forms of depositional and diagenetic calcite in hot-spring travertines, Central Italy. In: N. Schneidermann and P. M. Harris (eds), *Carbonate Cements*. Society for Sedimentary Geology Special Publication **36**, 349-379.
- Garden, I. R., Guscott, S. C., Burley, S. D., Foxford, K. A., Walsh, J. J. and Marshall, J. 2001. An exhumed palaeo-hydrocarbon migration fairway in a faulted carrier system, Entrada Sandstone of SE Utah, USA. *Geofluids* **1**. 195 – 214.
- Guerra, M. and Lombardi, S. 2001. Soil-gas method for tracing neotectonic faults in clay basins: the Pisticci field (Southern Italy). *Tectonophysics* **339**, 511-522.

Guo, L., Andrews, J., Riding, R., Dennis, P., Dresser, Q. 1996. Possible microbial effects on stable carbon isotopes in hot-spring travertines. *Journal of Sedimentary Research* **66**, 468-473.

Hancock, P.L., Chalmers, R.M.L., Altunel, E., Cakir, Z. 1999. Travertines; using travertines in active fault studies. *Journal of Structural Geology* **21**, 903-916.

Hansley, P.L. 1995. Diagenetic and burial history of the White Rim Sandstone in the Tar Sand Triangle, Paradox Basin, southeastern Utah. US Geological Survey Bulletin 2000-I, 41pp.

Heath J.E., Lachmar T.E., Shipton Z.K., Nelson, S. and Evans J.P., 2002.

Hydrogeochemical analysis of leaking CO₂-charged fault zones: the Little Grand Wash and Salt Wash fault zones, Emery and Grand counties, Utah. Geological Society of America Abstracts with Programs, v 34, # 6, p 392

Heath, J. E., 2004, Hydrogeochemical characterization of leaking Carbon dioxide-charged fault zones in east-central Utah, M. S. Thesis, Utah State University, Logan, 166 pp.

Hecker, S. 1993. Quaternary tectonics of Utah with emphasis on earthquake-hazard characterization. *Utah Geological Survey Bulletin* **127**, p. 157.

Hood, J.W. and Patterson, D.J. 1984. Bedrock aquifers in the northern San Rafael Swell area, Utah, with special emphasis on the Navajo Sandstone. State of Utah Department of Natural Resources Technical Publication no. 78.

IAEA (2001). GNIP Maps and Animations, International Atomic Energy Agency, Vienna. World Wide Web address: <http://isohis.iaea.org>

- Irwin, W.P. and Barnes, I. 1980. Tectonic relations of carbon dioxide discharges and earthquakes. *Journal of Geophysical Research* **85**, 3115-3121.
- Jenden P.D., Kaplan I.R., Poreda R.J., Craig H., 1988. Origin of nitrogen-rich natural gases in the California great valley - evidence from helium, carbon and nitrogen isotope ratios. *Geochimica et Cosmochimica Acta* 52 (4): 851-861
- Kirschner, D., Encarnacion, J., and Agosta, F. 2000. Incorporating stable isotope geochemistry in undergraduate laboratory courses. *Journal of Geoscience Education* **48**, 209-215.
- Mayo, A.L., Shrum, D.B. and Chidsey, T.C., Jr. 1991. Factors contributing to exsolving carbon dioxide in ground-water systems in the Colorado Plateau, Utah. In: Chidsey, T.C, Jnr. (eds) *Geology of east-central Utah*. Utah Geological Association Publication **19**, 335-342.
- McKnight, E.T. 1940. Geology of area between Green and Colorado rivers, Grand and San Juan Counties, Utah. U.S. Geological Survey Bulletin 908. 147 p.
- Mueller, B., Reinecker, J., Heidbach, O. and Fuchs, K. (2000): The 2000 release of the World Stress Map (available online at www.world-stress-map.org)
- Nuccio, V.F. and Condon, S.M. 1996. Burial and thermal history of the Paradox Basin, Utah and Colorado, and the petroleum potential of the Middle Pennsylvanian Paradox Formation. U.S. Geological Survey Bulletin 2000-O. 41pp.
- Peterson, P., R. 1973. Salt Wash field. Utah Geological Survey oil and gas field studies, no 4. 3pp.
- Pentecost, A. 1995. Geochemistry of carbon dioxide in six travertine-depositing waters of Italy. *Journal of Hydrology* **167**, 263-278.

- Pevear, D.R., Vrolijk, P.J. and Longstaffe, F.J. 1997. Timing of Moab fault displacement and fluid movement integrated with burial history using radiogenic and stable isotopes. In: Hendry, J., Carey, P., Parnell, J., Ruffel, A. and Worden, R. (eds) *Geofluids II 1997 Extended abstract volume*, 42-45.
- Powell, J. W., 1895. *The Canyons of the Colorado* (now published as *The exploration of the Colorado River and its canyons*. Penguin Books 1997. 416 pages)
- Rochelle, C.A., Pearce, J.M. and Holloway, S. 1999. The underground sequestration of carbon dioxide: containment by chemical reactions in the deep geosphere. In: Metcalfe, R. and Rochelle, C.A. (eds), *Chemical containment of waste in the lithosphere*, Geological Society, London, Special Publications, **157**, 117-129.
- Sanford, R.F. 1995. Groundwater flow and migration of hydrocarbons to the Lower Permian White Rim Sandstone, Tar Sand Triangle, Southeastern Utah. U.S. Geological Survey Bulletin 2000-J, 24pp.
- Schoell, M., 1983. Genetic characterization of natural gases. *American Association of Petroleum Geologists Bulletin*, **67**, 2225-2238.
- Selley, R.C., 1998. *Elements of Petroleum Geology*, 2nd ed., Academic Press. 470pp.
- Sugisaki, R. and seven others 1983. Origin of hydrogen and carbon dioxide in fault gases and its relation to fault activity. *Journal of Geology*, **91**, 239-258.
- Truesdell, A.H. and Jones, B.F. 1974, WATEQ, a computer program for calculating chemical equilibria of natural waters. *Journal of Research of the U. S. Geological Survey*. Pages 233-248.
- Williams, P.L. 1964, *Geology, structure, and uranium deposits of the Moab Quadrangle, Colorado and Utah*. U. S. Geological Survey Map I- 360.

Williams, P.L Hackman, R.J. 1971, Geology, structure, and uranium deposits of the Salina Quadrangle, Utah. U. S. Geological Survey Map I-591.

Wong, I. G., and Humphrey, J. R. 1989. Contemporary seismicity, faulting, and the state of stress in the Colorado Plateau. *Geological Society of America Bulletin*, **101**, 1127-1146

Zoback, M.D., and Townend, J. 2001, Implications of hydrostatic pore pressure and high crustal strength for the deformation of intraplate lithosphere. *Tectonophysics*, **336** 19-30.

Figure captions

Figure 1. a) Regional geology of the Little Grand Wash and Salt Wash faults. Stars mark the location of known CO₂-charged springs. Dot marks the town of Green River, Utah. Compiled from Doelling 2001; Williams 1964; Williams and Hackman 1971. The line of section shown in Figure 2 is indicated. Inset shows location of study area and approximate boundaries of the Paradox Basin. b) Stratigraphic column. (after Doelling, 2001). Stippled areas indicate likely reservoir or aquifer rocks, cross hatched areas represent likely cap rocks or seals.

Figure 2. Schematic cross-section across the Little Grand Wash and Salt Wash faults, approximately along the north-plunging anticline axis. Depths are above or below seal level. Abandoned oil wells (projected onto the line of section) give control on the stratigraphy. The structure of the Salt Wash faults is not constrained at depth by any well data. The line of section is indicated on Figure 1.

Figure 3. Local map of the Little Grand Wash fault showing the location of the travertine deposits, the gas seep, oil seep, and abandoned oil wells mentioned in the text.

Figure 4. Photos of Little Grand Wash fault. a) Cross-sectional view looking east along fault strike, about 30 m east of Crystal Geyser. At this location the fault consists of several strands separating structural terraces. The southern fault strand accommodates most of the offset here. Note the thick calcite/aragonite veins cutting the travertine that sits in the hangingwall of the central fault strand. Js = Jurassic Summerville Formation, Kmu = Cretaceous Mancos Shale. Photo about 500 m across. b) Boxwork of veins beneath a travertine mound centred on the northern fault strand. Note that the fault does not clearly cut all the way up the travertine mound, and appears to be cut by some of the veins. The host rocks are Jurassic Morrison Formation, Jmb = Brushy Basin shale member, Jms = Salt Wash sandstone member. Three people in the centre for scale.

Figure 5. a) Eruption of the Crystal Geyser looking east along fault. Active and inactive travertine mounds can be seen around geyser, and ancient travertine mounds and carbonates are located along fault surface. Strands of fault are marked. Je = Entrada Formation, Jct = Curtis Formation, Js = Summerville Formation, Jms = Salt Wash Sandstone (Morrison Formation), Jmb = Brushy Basin member of Morrison Formation, Kmu = Mancos Shale. b) Thick veins cutting the lower inactive travertine mound at the edge of the Green River. Veins dip into mound, but roll over to subvertical at front of photo. Top of this mound consists of a breccia with clasts of vein material. Modern travertine deposits are covering the ancient mound in bottom left of photo. This section is about 2 m high.

Figure 6. Map of Salt Wash fault outcrops mentioned in text. Locations of springs and travertine/carbonate vein deposits are marked including ones not specifically mentioned in text. Abandoned oil wells are shown with their total depth (TD) and depth to top of the Paradox salt.

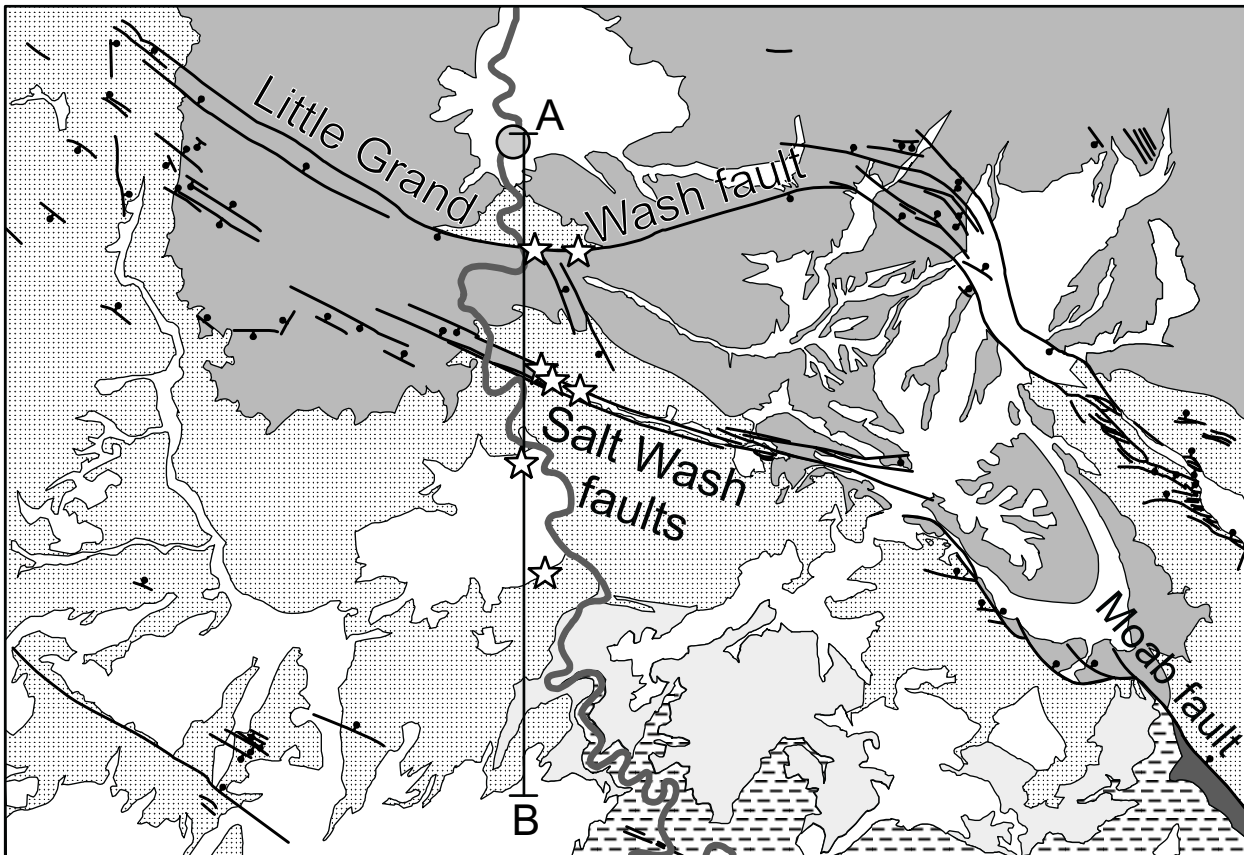
Figure 7. Photos of Salt Wash fault. a) Aerial view of northern Salt Wash fault looking north, showing distribution of springs and travertines in vicinity of Tenmile Geyser. b) Cross-sectional view looking east along fault strike, about 800 m west of Tenmile Geyser. At least three fault strands, consisting of thin gouge zones, can be identified based on differing lithologies. c) Alteration focussed along fractures and bedding planes adjacent to fault zone. At top of outcrop the base of an ancient travertine mound can be seen. Je = Entrada Formation, Js = Summerville Formation, Jms = Salt Wash Sandstone (Morrison Formation), Jmb = Brushy Basin member of the Morrison Formation, Kcm = Cedar Mountain Formation.

Figure 8. Variation in sodium (dotted lines) and potassium (solid lines) concentrations from the Crystal Geyser during two separate eruptions (time from start of eruption in

minutes along x-axis). The squares show data from an eruption that lasted 30 minutes, the diamonds show data from an eruption that lasted less than 15 minutes.

Figure 9. Stable isotope data for travertines and ray-crystal calcite/aragonite veins analysed in this study, and for travertines and associated spring waters from published data. a) $\delta^{13}\text{C}$ (PDB) vs. $\delta^{18}\text{O}$ (SMOW) for samples of veins (solid symbols) and travertines (unfilled symbols) at the Little Grand Wash and Salt Wash faults.

Differences between veins and travertine at individual localities could be due either to decrease in temperature when fluids evolve onto land surface or different sources of fluid. Vertical arrays formed by travertine data are consistent with progressive CO_2 degassing during surface flow of water. b) Vertical data arrays of travertine and travertine-forming spring waters in $\delta^{13}\text{C}$ - $\delta^{18}\text{O}$ space are common and result from downstream CO_2 degassing of spring water, seasonal variations in isotopic values of source waters, and variable microbial influence in facilitating the precipitation of travertine carbonates. All six studies are from active travertine deposits: (1) Mammoth Hot Springs, Yellowstone (Friedman, 1970), spring temperature in $^{\circ}\text{C}$; (2) Durango, Colorado (Chafetz *et al.*, 1991a); (3) Oklahoma (Chafetz *et al.*, 1991b); (4) Coast Range, California (Amundson and Kelley, 1987); (5) near Florence, Italy (Guo *et al.*, 1996); (6) Central Italy (Pentecost, 1995).



	Formation	Member	symbol	thickness (m)
Cretaceous	Mancos Shale	U. member	Kmu	915
		Ferron Sst	Km	3-9
		Tununk	Kmt	107-1220
	Dakota Sandstone		Kd	0-10
	Cedar Mountain Fm.		Kcm	46-55
Jurassic	Morrison Formation	Brushy Basin	Jmb	73-128
		Salt Wash	Jms	49-88
		Tidwell	Jmt	6-15
	Summerville Fm.		Js	30-122
	Curtis Sandstone		Jct	40-70
	Entrada Sandstone		Je	125-143
	Carmel Formation		Jc	67-91
	Glen Canyon Gp.	Navajo Sandstone	Jn	131-155
		Kayenta Formation	Jk	58-73
		Wingate Sandstone	Jw	91-122
Triassic	Chinle Formation	TRc	79-165	
	Moenkopi Formation	TRm	204-277	
Permian	Black Box Dolomite	Pb	18-49	
	Cutler Gp.	White Rim	Pcw	91-152
		Organ Rock	Pco	0-91
Pennsylvanian	Hermosa Gp.	Honaker Trail Form.	Ph	152-305
		Paradox Formation	Pp	305-762

